HHS Public Access

Author manuscript

Oncogene. Author manuscript; available in PMC 2010 October 29.

Published in final edited form as:

Oncogene. 2010 April 29; 29(17): 2477–2487. doi:10.1038/onc.2010.10.

Pim1 kinase synergizes with c-MYC to induce advanced prostate carcinoma

Jie Wang[1], **Jongchan Kim**[2], **Meejeon Roh**[2], **Omar E. Franco**[3], **Simon W. Hayward**[1,3], **Marcia L. Wills**[2], and **Sarki A. Abdulkadir**[1,2]

[1]Department of Cancer Biology, Vanderbilt University Medical Center, Nashville, TN 37232, USA

[2]Department of Pathology, Vanderbilt University Medical Center, Nashville, TN 37232, USA

[3]Department of Urology, Vanderbilt University Medical Center, Nashville, TN 37232, USA

Abstract

The oncogenic PIM1 kinase has been implicated as a cofactor for c-MYC in prostate carcinogenesis. Here we show that in human prostate tumors, coexpression of c-MYC and PIM1 is associated with higher Gleason grades. Using a tissue recombination model coupled with lentiviral-mediated gene transfer we find that Pim1 is weakly oncogenic in naïve adult mouse prostatic epithelium. However, it cooperates dramatically with c-MYC to induce prostate cancer within 6-weeks. Importantly, c-MYC/Pim1 synergy is critically dependent on Pim1 kinase activity. c-MYC/Pim1 tumors showed increased levels of the active serine-62 (S62) phosphorylated form of c-MYC. Grafts expressing a phosphomimetic c-MYCS62D mutant had higher rates of proliferation than grafts expressing wild type c-MYC but did not form tumors like c-MYC/Pim1 grafts, indicating that Pim1 cooperativity with c-MYC *in vivo* involves additional mechanisms other than enhancement of c-MYC activity by S62 phosphorylation. c-MYC/Pim1-induced prostate carcinomas demonstrate evidence of neuroendocrine (NE) differentiation. Additional studies, including the identification of tumor cells coexpressing androgen receptor and NE cell markers synaptophysin and Ascl1 suggested that NE tumors arose from adenocarcinoma cells through transdifferentiation. These results directly demonstrate functional cooperativity between c-MYC and PIM1 in prostate tumorigenesis *in vivo* and support efforts for targeting PIM1 in prostate cancer.

Keywords

Pim1; c-MYC; prostate cancer; mouse model; neuroendocrine

Introduction

An important area in contemporary cancer research is defining the causative genetic alterations in tumors and their utility as molecular targets. In this regard, gene expression

*Request for reprints: Sarki A. Abdulkadir, Department of Pathology, Vanderbilt University Medical Center, B-3321A MCN, 1161 21st Avenue South, Nashville, TN 37232, 615-322-9668 (tel); 615-343-7023 (fax), sarki.abdulkadir@vanderbilt.edu.

profiling studies have identified overexpression of the serine-threonine kinase PIM1 in a significant fraction of human prostate tumors where its expression is found to be tightly associated with that of c-MYC (hereafter, MYC) (Dhanasekaran et al., 2001; Ellwood-Yen et al., 2003; Valdman et al., 2004). Pim1 is also overexpressed in Myc-driven transgenic mouse prostate tumors and Pim1 overexpression increases the tumorigenicity of human prostate cancer cell lines (Ellwood-Yen et al., 2003), (Bhattacharya et al., 2002; Chen et al., 2005; Roh et al., 2008; Roh et al., 2005). Previous studies in mouse lymphoma models have shown that Pim1 and Myc synergize to promote lymphomagenesis (van Lohuizen et al., 1989).

Pim1 is able to interact and phosphorylate several targets that are involved in cell cycle progression or apoptosis. Pim1 can inhibit apoptosis through interactions with the anti-apoptotic molecules, bcl-2 and Gfi-1 (Schmidt et al., 1998) or by inactivating phosphorylation of Bad at serine 112 (Aho et al., 2004). Substrates of Pim1 involved in cell cycle regulation include $p21^{Cip1}$ (Wang et al., 2002), $p27^{Kip1}$ (Morishita et al., 2008), NuMA (Bhattacharya et al., 2002), Cdc25A (Mochizuki et al., 1999), Cdc25c (Bachmann et al., 2006) and c-TAK1 (Bachmann et al., 2004). Recent studies showed that Myc recruits Pim1 to the E boxes of Myc target genes where Pim1-dependent phosphorylation of histone H3 on serine 10 contributes to the activation of Myc target genes and cellular transformation (Zippo et al., 2007). Other studies suggest that Pim1 can phosphorylate c-Myc and inhibit its degradation (Zhang et al., 2008). All of these observations suggested the possibility that Pim1 may cooperate with Myc in prostate tumorigenesis. However, whether Pim1 does cooperate with c-Myc in prostate tumorigenesis *in vivo* has to our knowledge not been conclusively demonstrated.

In this report, we first showed that coexpression of MYC and PIM1 in human prostate cancer samples correlated with tumor grade. Then we used a tissue recombination model to directly examine cooperativity between MYC and Pim1 in prostate tumorigenesis and the possible role of Pim1 kinase activity in this process. Our results revealed a potent synergy between Pim1 and MYC in prostate tumor development that is critically dependent on Pim1 kinase activity.

Materials and Methods

Lentiviral constructs

We generated lentiviral constructs coexpressing YFP and mouse Pim1, Pim1 kinase-dead mutant K67M (Roh et al., 2003), human c-MYC or c-MYCS62D. Additional details are provided in the Supplementary Methods.

Tissue recombination

All lobes of prostates were isolated from 6 week old C57BL/6 mice, minced and digested with collagenase (Gibco-BRL) at 37°C for 90 min. A single cell suspension was generated using Trypsin, Dispase and DNase I, and passed through 100μm nylon mesh (BD Biosciences). Dissociated prostate cells were infected with lentivirus at MOI 50–100 in the presence of 8 μg/ml polybrene using the centrifugation method (Xin et al., 2003). Rat fetal

urogenital mesenchyme (UGM) was prepared from 18-day embryos. Urogenital sinuses were dissected from fetuses and separated into epithelial and mesenchymal components by tryptic digestion as described previously (Hayward et al., 1998). Single cells of UGM were then prepared by a 90-min digestion at 37°C with 187 units/ml collagenase. 2×10^5 cells were recombined with 2.5×10^5 rat urogenital mesenchyme (UGM) and suspended in rat tail collagen prepared as described (Hayward et al., 1998). The recombinants were incubated overnight and subsequently placed beneath the renal capsule of male SCID mice. Six or 12 weeks after grafting, the hosts were sacrificed. Animal experiments were performed according to protocols approved by the Institutional Animal Care and Use Committee at Vanderbilt University.

Histology and Immunohistochemistry

Histological and immunohistochemical analyses were performed as described (Abdulkadir et al., 2001a; Abdulkadir et al., 2001b). Details of antibodies are in the Supplementary Methods. For Ki67 and activated caspase3 quantitation, we counted at least 1000 cells per graft. For human prostate tumors samples, tissue arrays from Imgenex were stained by double immunofluorescence for MYC (Santa Cruz Biotechnology, 1:15,000 with Tyramide Signal Amplification) and PIM1 (Santa Cruz Biotechnology, 1:50) as described (Kim et al., 2009). Coexpression was scored in samples where at least 50% of the cells coexpressed both antigens. Epithelial staining intensity was scored where ≥ 5% of cells show staining on a 4-point scale (0=negative, 1=weak, 2=intermediate, 3=strong) and samples were categorized as either not overexpressing (scores 0, 1) or overexpressing (scores 2, 3) the antigen. Tissue histology was confirmed by H&E staining.

Western blot analyses

These were performed as described previously (Roh et al., 2003) using the following antibodies: c-MYC, Pim1, AR, β-actin (Santa Cruz Biotechnology, 1:500); Cyclins D1, D2 , E (Santa Cruz Biotechnology, 1:1000**);** c-MYC phospho S62 (Abcam, 1:1000).

Statistical analysis

We compared groups by using t-test or Chi-square test (http://www.quantpsy.org). Values were considered statistically significant at $P < 0.05$. Quantitative variables are expressed as means ± SD while categorical variables are expressed as numbers (%).

Results

Co-expression of c-MYC and Pim1 in human prostate cancer

To examine co-expression of MYC and PIM1 proteins in human prostate tumors, we employed immunohistochemical analysis of tissue microarrays (TMAs) from total prostatectomy specimens. Out of 91 specimens examined, MYC staining was observed in 52 (57%) cases and PIM1 staining was present in 58 (64%). There was considerable overlap between samples that express MYC and PIM1 (44.4%) (Fig. 1A, B). In addition, coexpression of c-MYC and PIM1 was significantly correlated to higher Gleason grades. Of 28 samples with Gleason grade 4/5, seventeen (61%) were MYC/PIM1 double-positive (Fig. 1C). These results are consistent with, and extend previous findings that MYC and PIM1

mRNA are frequently coexpressed in human prostate tumors (Dhanasekaran et al., 2001; Ellwood-Yen et al., 2003).

Pim1 and MYC synergize to accelerate prostate cancer progression

To study the effects of MYC and Pim1 on naïve mouse prostate epithelium, we employed tissue recombination with lentiviral-mediated gene transfer (Cunha & Lung, 1978; Xin et al., 2003). We first generated lentiviruses expressing Pim1, K67M (kinase-dead Pim1 mutant) and MYC as well as yellow fluorescent protein (YFP) variant, Venus (Fig. 2A, Fig. S1). We then infected dissociated prostate cells from 6-week old C57BL/6 mice with the control, Pim1, K67M or MYC-expressing lentiviruses singly or in combination (MYC/Pim1 or MYC/K67M). Cells were combined with rat urogenital sinus mesenchyme (UGM) and grafted under the renal capsules of SCID mice to regenerate prostates (Fig. 2B). After six weeks, gross examination showed that the MYC/Pim1 grafts had formed large hemorrhagic tumors while control, or Pim1, or K67M, or MYC and MYC/K67M grafts were small and did not differ significantly in their sizes (Fig. 2C). Western blot confirmed appropriate transgene expression (Fig. 2D). In MYC/Pim1 tumors, the protein levels of MYC and Pim1 appear elevated, which may be due to the increased cellularity of tumors or other mechanisms such as reduced protein degradation. It is known that both MYC and PIM1 have a short half-life (Saris et al., 1991; Yeh et al., 2004) and Pim1 inhibits MYC degradation in a kinase-dependent manner (Zhang et al., 2008). Histologically, all grafts from control (N=7), Pim1 (N=8) or K67M (N=8) group consisted of normal-looking prostatic glands (Fig. 3A). Thus, Pim1 expression does not lead to a discernible pathology, consistent with it being a weak oncogene. By contrast, all MYC (N=19) and MYC/K67M (N=11) grafts showed multiple foci of high-grade PIN (HGPIN), a putative precursor lesion for prostate carcinoma. These lesions are characterized by nuclear pleomorphism, prominent nucleoli, high mitotic activity, apoptotic figures and stromal hypercellularity. None of the MYC or MYC/K67M 6-week grafts showed evidence of invasive cancer (Fig. 3A).

Strikingly, MYC/Pim1 grafts (N=13) consisted of prostate tumors growing as sheets of cells with notable rosette formation upon histological examination. The tumor cells have bubbly cytoplasm, vesicular nuclei, high nuclear:cytoplasmic ratios, large nuclei and prominent nucleoli (Fig. 3A). These tumors are also highly vascular. Histologically, these tumors are consistent with neuroendocrine carcinomas and look similar to human prostate neuroendocrine or small cell carcinoma (Fig. 3B). We observed a single mouse that died of metastatic carcinoma in the sixth week. These results indicate potent cooperation between MYC and Pim1 in prostate tumorigenesis which is critically dependent on Pim1 kinase activity.

MYC/Pim1 tumors show high rates of proliferation, apoptosis and evidence of enhanced MYC function

The Pim1 kinase may inhibit apoptosis via interactions with the anti-apoptotic molecules, Bcl-2 and Gfi-1 (Schmidt et al., 1998) or by phosphorylation of the pro-apoptotic protein Bad at serine 112 (Aho et al., 2004). On the other hand, Pim1 has also been reported to promote c-Myc mediated apoptosis in serum-deprived Rat-1 fibroblasts (Mochizuki et al., 1999). It is speculated that Pim1 cooperates with Myc by inhibiting the apoptotic effect of

Myc. We examined proliferation and apoptosis using immunohistochemical staining. Notably, the rates of proliferation (Ki-67 index) and apoptosis (activated caspase 3 index) were similarly low in the 6-week control, Pim1 and K67M grafts, consistent with the absence of histological alterations in those samples. However, there were significant increases in proliferation and apoptosis in the MYC grafts and similar increases were noted in the MYC/K67M group relative to control. The Ki67-index was dramatically increased in the MYC/Pim1 tumors consistent with the high-grade nature of these cancers. The apoptotic index was also similarly elevated indicating high turnover of the tumor cells (Fig. 4A, B). The increased apoptosis in the MYC/Pim1 tumors may indicate high cell turnover due to the markedly elevated rates of proliferation. Since there were many more cells undergoing proliferation than apoptosis, the net effect was increased tumor growth.

Reports indicate that Pim1 may enhance MYC activity by increasing the phosphorylation of MYC on serine-62 (MYCS62P) leading to enhanced stability and transcriptional activity (Chen et al., 2005; Zhang et al., 2008). Other studies have shown that Pim1 phosphorylation of histone H3 on serine-10 facilitates transcriptional activation by MYC (Zippo et al., 2007). Based on these studies, it is expected that MYC activity will be enhanced in MYC/Pim1-expressing tumors. In agreement with this notion, we found that relative levels of MYC and its targets cyclins D1, D2, E were elevated in MYC/Pim1 tissues comparing those in MYC or MYC/K67M grafts (Fig. 4C, D). Furthermore, MYCS62P levels normalized to total MYC protein levels were higher in MYC/Pim1 tumors than MYC or MYC/K67M grafts (Fig. 4E).

To directly assess the contribution of MYC phosphorylation on serine-62 to tumorigenic activity *in vivo*, we generated grafts using lentiviruses expressing the MYCS62D (serine-to-aspartic acid) phosphomimetic mutant or wild type MYC (n=4–5). Histological examination revealed no significant differences between MYC and MYCS62D grafts. Both showed HGPIN with no evidence of invasive cancer as confirmed by SMA staining (Fig. 4E). To assess rates of proliferation, we co-stained the graft sections with phospho-histone H3 (a mitotic marker) and MYC so that we can determine the mitotic index in MYC-expressing cells. This analysis revealed a significantly higher mitotic index in the MYCS62D grafts than MYC grafts (Fig. 4F). Overall, these results indicate that although MYCS62 phosphorylation does enhance the pro-proliferative effects of MYC, this mechanism does not account for the bulk of the cooperativity between MYC and Pim1 in our system.

Evidence of neuroendocrine differentiation in MYC/Pim1 tumors

To characterize the cell types present in the regenerated grafts, we performed an immunohistochemical analysis using a panel of cellular markers including androgen receptor (AR), Nkx3.1, E-cadherin, CK8, p63, smooth muscle actin (SMA), synaptophysin, ‘archaete-scute complex’ homolog 1 (Ascl1), neuron-specific enolase (NSE), and the forkhead transcription factor FoxA2. Control, Pim1 and K67M-expressing grafts showed identical staining patterns for all of these markers (Fig. 5, Fig. S2 and data not shown). This is consistent with the absence of discernible pathology in 6-week Pim1 or K67M-expressing grafts (Fig. 3). The HGPIN lesions in MYC or MYC/K67M grafts showed identical patterns of biomarker expression. Notably, the MYC and MYC/K67M grafts were strongly positive

for smooth muscle actin staining in the surrounding hypercellular stroma (Fig. 5). The hypercellular stroma does not appear to be due to stromal expression of MYC as determined by immunohistochemistry (Fig. S3). Stromal reaction has been noted in association with HGPIN lesions in several mouse models of prostate cancer (Shappell et al., 2004).

Examination of MYC/Pim1 tumors showed low AR expression, loss of E-cadherin, p63, CK8 and SMA (Fig. 5), consistent with an invasive phenotype. These tumors ubiquitously expressed the NE marker synaptophysin (Fig. 5). Further analysis showed that these tumors also expressed the neurogenic transcription factor Ascl1 (Hu et al., 2004) (Vias et al., 2008) (Fig. 7). We also noted heterogeneous expression of neuron-specific enolase (di Sant'Agnese & de Mesy Jensen, 1987) (Fig. S2). The tumors did not express prostate differentiation marker and tumor suppressor Nkx3.1 (Abdulkadir et al., 2002) or FoxA2, which is expressed in some neuroendocrine tumors (Mirosevich et al., 2006) (Fig. S2). These results demonstrate that MYC/Pim1 coexpression leads to the development of high-grade cancer with features of NE differentiation within 6 weeks.

Chronic Pim1 overexpression leads to the development of low grade PIN lesions

To examine the effect of chronic overexpression of Pim1, we allowed grafts to grow for 12 weeks. While grafts from the kinase-dead mutant K67M (N=4), which were used as controls here, consisted of normal glands, Pim1-expressing grafts showed focal epithelial hyperplasia and dysplasia consistent with low grade PIN (N=4) (Fig. 6A; see Fig. 3B for comparison to human LGPIN). Ki67 staining showed a slight elevation of the Ki67-index in Pim1 grafts compared to K67M grafts, but did not reach statistical significance, while both the Pim1 and K67M grafts showed low levels of apoptosis (Fig. 6C). Pim1 has been reported to interact with and phosphorylate several cell cycle and apoptotic molecules, including Cdc25A/C, C-TAK1, $p21^{cip1}$, $p27^{kip1}$ and Bad (Bachmann & Moroy, 2005; Morishita et al., 2008). Accordingly, Pim1 is proposed to promote proliferation and inhibit apoptosis. The lack of a discernible phenotype after 6 weeks of Pim1 overexpression suggests that the homeostatic mechanisms operating in prostatic cells are able to buffer the effects of Pim1 overexpression. At 12 weeks, we speculate that a small reduction in the rate of apoptosis in Pim1 grafts coupled with a modest increase in proliferation could account for accumulation of epithelial cells manifesting as hyperplasia.

Chronic c-MYC overexpression results in adenocarcinoma and carcinoma with neuroendocrine differentiation

Consistent with the notion that Pim1 accelerates MYC-initiated tumors, by 12 weeks, grafts expressing MYC alone produced synaptophysin-positive neuroendocrine tumors and adenocarcinoma with focal synaptophysin-positive cells (Fig. 6A, B). The 12-week MYC neuroendocrine tumors expressed low levels of AR by western blot (Fig. 6D) and immunohistochemical staining (Fig. S4). Neuroendocrine prostate cancer may arise directly from the transformation of rare neuroendocrine cells in the prostate or via the transdifferentiation of adenocarcinoma (Cindolo et al., 2007). If the neuroendocrine tumor arose from the transformation of neuroendocrine cells, one would expect to see clusters of neuroendocrine cells in precursor HGPIN lesions. However, we did not observe clusters of synaptophysin positive cells in the HGPIN lesions from any MYC or MYC/Pim1 samples.

Instead, we found foci of synaptophysin-positive cells in invasive adenocarcinoma lesions as mentioned (Fig. 6B). Therefore, the neuroendocrine tumors that developed due to co-expression of MYC/Pim1 or the chronic overexpression of MYC probably arose via the transdifferentiation of adenocarcinoma to a neuroendocrine phenotype. Further evidence for this hypothesis was obtained by identification of cells that coexpress AR, MYC and the NE markers synaptophysin and Ascl1 in MYC/Pim1 tumors (Fig. 7). These results are consistent with recent data from human tumors where careful analysis revealed evidence of transdifferentiation from adenocarcinoma to neuroendocrine cancer (Hansel et al., 2009; Sauer et al., 2006; Wafa et al., 2007).

Additional analysis of 12-week MYC grafts showed levels of proliferation and apoptosis consistent with tumor grade, with the neuroendocrine tumors showing the highest rates of proliferation and apoptosis (Fig. 6C). Interestingly, Western blot analysis of the 12-week grafts showed overexpression of endogenous Pim1 in synaptophysin-positive MYC tumors (Fig. 6D), suggesting that with progression, MYC tumors select for Pim1 overexpression, or Pim1 may be induced by neuroendocrine tumor secreted factors. These results are consistent with previous observations of Pim1 mRNA overexpression in Probasin-Myc transgenic tumors although those tumors were not reported to express markers of NE differentiation (Ellwood-Yen et al., 2003). On the other hand, Pim1 and L-Myc were reported to be up-regulated in neuroendocrine prostate tumors induced by combined deletion of p53 and Rb in mice (Zhou et al., 2006).

Discussion

In humans, PIM1 and MYC levels are upregulated, which suggests they cooperate in prostate tumorigenesis. In this study, we found that a significant percentage of the human prostate cancer samples exhibited concurrent overexpression of MYC and PIM1, which is associated with higher Gleason grades. Therefore, we examined the effects of MYC and Pim1 overexpression in prostate carcinogenesis using a tissue recombination model. Our study has provided several insights. We demonstrated that Pim1 by itself is weakly oncogenic, consistent with previous results in lymphoma models. However, Pim1 synergizes dramatically with MYC to promote the development of advanced prostate carcinoma. Our results also demonstrate a strict requirement for Pim1 kinase activity for both its oncogenic activity and its ability to synergize with MYC.

One model of how Pim1 cooperates with MYC in transformation is by enhancing MYC transcriptional activity at various levels. These include by altering MYC phosphorylation to affect activity and stability, as well as by via modification of chromatin at MYC binding sites. We have been able, in this report, to explore the relative contribution of MYC S62 phosphorylation to the generation of tumors by using lentivirus expressing the phosphomimetic MYCS62D mutant. Our results indicate that while expression of the MYCS62D mutant did increase proliferation by approximately 2-fold, it failed to recapitulate the advanced tumor phenotype observed by coexpressing MYC and Pim1. Further studies are warranted to further dissect the mechanisms by which MYC and PIM1 cooperate in prostate carcinogenesis.

Tumors derived from the co-expression of MYC and Pim1 show evidence of neuroendocrine differentiation. Pure neuroendocrine or small cell carcinoma of the prostate is rare, and has a poor prognosis. However, partial neuroendocrine differentiation in prostate cancer, defined as expression of one or more neuroendocrine markers such as chromogranin A, synaptophysin, neuron specific enolase, L-dopa carboxylase, is more common and is associated with a poor prognosis (Hansel et al., 2009; Sauer et al., 2006; Wafa et al., 2007; Yuan et al., 2007). There is also extensive literature on the transdifferentiation of prostate adenocarcinoma to neuroendocrine phenotype. For example, LNCaP human prostate carcinoma cells can be induced to transdifferentiate to NE-like cells by androgen depletion, interleukin-6 treatment or genistein treatment (Deeble et al., 2001; Kim et al., 2002; Pinski et al., 2006; Zhang et al., 2003). Our findings support the notion that the MYC/Pim1 tumors arise from transdifferentiation of adenocarcinoma cells to acquire neuroendocrine features rather than from the transformation of the rare neuroendocrine cell type in the prostate. First, prostate tissue recombinants are derived from adult mouse prostate cells by prostate regeneration. If rare neuroendocrine cells were transformed by oncogene expression, one would expect to see clusters of transformed neuroendocrine cells in early lesions. However, we have never observed clusters of transformed neuroendocrine cells in precursor PIN lesions. This is in contrast to the situation in which neuroendocrine cells are transformed, such as targeted expression of T antigen in the Cr2-TAg model. In Cr2-TAg mice, transformed neuroendocrine cell clusters are readily identified in PIN lesions (Abdulkadir et al., 2001b; Garabedian et al., 1998). Secondly, we were able to identify cells coexpressing both AR and synaptophysin, consistent with transdifferentiation of adenocarcinoma cells to neuroendocrine cancer, similar to recent observations in some human prostate tumors (Wafa et al., 2007) as well as in TRAMP mice (Kaplan-Lefko et al., 2003). Our findings are reminiscent of observations made on a neuroendocrine model of prostate cancer due to prostate-specific deletion of *Trp53* and *Rb* (Zhou et al., 2006). Tumors from this model were found to coexpress synaptophysin and androgen receptor and to upregulate the proneural transcription factors Ascl1 and Hes6 (Vias et al., 2008). Interestingly, the expression of pro-neural transcription factors was useful in segregating metastatic from localized prostate cancer (Vias et al., 2008).

Our findings clearly show that Pim1 kinase activity is important for the synergy between Pim1 and MYC in prostate carcinogenesis. The Pim1 has recently garnered interest as a possible molecular target in multiple cancers including lymphomas and prostate cancer. Mice deficient in Pim1 or all Pim kinases (Pim1/Pim2/Pim3) showed a very mild phenotype, suggesting that therapeutic inhibition of Pim1 may be well tolerated. Our results also suggest that Pim1 kinase inhibitor may be an effective strategy against prostate cancer progression. Our MYC/Pim1 tissue recombination model may be useful for testing therapeutic modalities aimed at inhibiting Pim1 as it avoids both the drawbacks of xenografts that use advanced cancer cell lines as well as the cost/time constraints that hamper most transgenic models.

Supplementary Material

Refer to Web version on PubMed Central for supplementary material.

Acknowledgements

We thank Drs. Robert Matusik, Vito Quaranta, Fritz Parl and Susan Kasper for helpful discussions. This work was supported by NIH grant CA123484 (S.A.A.). The funders had no role in study design, data collection and analysis, decision to publish, or preparation of the manuscript.

References

Abdulkadir SA, Carbone JM, Naughton CK, Humphrey PA, Catalona WJ, Milbrandt J. Hum Pathol. 2001a; 32:935–939. [PubMed: 11567222]

Abdulkadir SA, Magee JA, Peters TJ, Kaleem Z, Naughton CK, Humphrey PA, Milbrandt J. Mol Cell Biol. 2002; 22:1495–1503. [PubMed: 11839815]

Abdulkadir SA, Qu Z, Garabedian E, Song SK, Peters TJ, Svaren J, Carbone JM, Naughton CK, Catalona WJ, Ackerman JJ, Gordon JI, Humphrey PA, Milbrandt J. Nat Med. 2001b; 7:101–107. [PubMed: 11135623]

Aho TL, Sandholm J, Peltola KJ, Mankonen HP, Lilly M, Koskinen PJ. FEBS Lett. 2004; 571:43–49. [PubMed: 15280015]

Bachmann M, Hennemann H, Xing PX, Hoffmann I, Moroy T. J Biol Chem. 2004; 279:48319–48328. [PubMed: 15319445]

Bachmann M, Kosan C, Xing PX, Montenarh M, Hoffmann I, Moroy T. Int J Biochem Cell Biol. 2006; 38:430–443. [PubMed: 16356754]

Bachmann M, Moroy T. Int J Biochem Cell Biol. 2005; 37:726–730. [PubMed: 15694833]

Bhattacharya N, Wang Z, Davitt C, McKenzie IF, Xing PX, Magnuson NS. Chromosoma. 2002; 111:80–95. [PubMed: 12111331]

Chen WW, Chan DC, Donald C, Lilly MB, Kraft AS. Mol Cancer Res. 2005; 3:443–451. [PubMed: 16123140]

Cindolo L, Cantile M, Vacherot F, Terry S, de la Taille A. Urol Int. 2007; 79:287–296. [PubMed: 18025844]

Cunha GR, Lung B. J Exp Zool. 1978; 205:181–193. [PubMed: 681909]

Deeble PD, Murphy DJ, Parsons SJ, Cox ME. Mol Cell Biol. 2001; 21:8471–8482. [PubMed: 11713282]

Dhanasekaran SM, Barrette TR, Ghosh D, Shah R, Varambally S, Kurachi K, Pienta KJ, Rubin MA, Chinnaiyan AM. Nature. 2001; 412:822–826. [PubMed: 11518967]

di Sant'Agnese PA, de Mesy Jensen KL. Hum Pathol. 1987; 18:849–856. [PubMed: 3610135]

Ellwood-Yen K, Graeber TG, Wongvipat J, Iruela-Arispe ML, Zhang J, Matusik R, Thomas GV, Sawyers CL. Cancer Cell. 2003; 4:223–238. [PubMed: 14522256]

Garabedian EM, Humphrey PA, Gordon JI. Proc Natl Acad Sci U S A. 1998; 95:15382–15387. [PubMed: 9860977]

Hansel DE, Nakayama M, Luo J, Abukhdeir AM, Park BH, Bieberich CJ, Hicks JL, Eisenberger M, Nelson WG, Mostwin JL, De Marzo AM. Prostate. 2009; 69:603–609. [PubMed: 19125417]

Hayward SW, Haughney PC, Rosen MA, Greulich KM, Weier HU, Dahiya R, Cunha GR. Differentiation. 1998; 63:131–140. [PubMed: 9697307]

Hu Y, Wang T, Stormo GD, Gordon JI. Proc Natl Acad Sci U S A. 2004; 101:5559–5564. [PubMed: 15060276]

Kaplan-Lefko PJ, Chen TM, Ittmann MM, Barrios RJ, Ayala GE, Huss WJ, Maddison LA, Foster BA, Greenberg NM. Prostate. 2003; 55:219–237. [PubMed: 12692788]

Kim J, Adam RM, Freeman MR. Cancer Res. 2002; 62:1549–1554. [PubMed: 11888934]

Kim J, Eltoum IE, Roh M, Wang J, Abdulkadir SA. PLoS Genet. 2009; 5:e1000542. [PubMed: 19578399]

Mirosevich J, Gao N, Gupta A, Shappell SB, Jove R, Matusik RJ. Prostate. 2006; 66:1013–1028. [PubMed: 16001449]

Mochizuki T, Kitanaka C, Noguchi K, Muramatsu T, Asai A, Kuchino Y. J Biol Chem. 1999; 274:18659–18666. [PubMed: 10373478]

Morishita D, Katayama R, Sekimizu K, Tsuruo T, Fujita N. Cancer Res. 2008; 68:5076–5085. [PubMed: 18593906]

Pinski J, Wang Q, Quek ML, Cole A, Cooc J, Danenberg K, Danenberg PV. Prostate. 2006; 66:1136–1143. [PubMed: 16652383]

Roh M, Franco OE, Hayward SW, van der Meer R, Abdulkadir SA. PLoS ONE. 2008; 3:e2572. [PubMed: 18596907]

Roh M, Gary B, Song C, Said-Al-Naief N, Tousson A, Kraft A, Eltoum IE, Abdulkadir SA. Cancer Res. 2003; 63:8079–8084. [PubMed: 14678956]

Roh M, Song C, Kim J, Abdulkadir SA. J Biol Chem. 2005; 280:40568–40577. [PubMed: 16221667]

Saris CJ, Domen J, Berns A. Embo J. 1991; 10:655–664. [PubMed: 1825810]

Sauer CG, Roemer A, Grobholz R. Prostate. 2006; 66:227–234. [PubMed: 16173029]

Schmidt T, Karsunky H, Rodel B, Zevnik B, Elsasser HP, Moroy T. Embo J. 1998; 17:5349–5359. [PubMed: 9736613]

Shappell SB, Thomas GV, Roberts RL, Herbert R, Ittmann MM, Rubin MA, Humphrey PA, Sundberg JP, Rozengurt N, Barrios R, Ward JM, Cardiff RD. Cancer Res. 2004; 64:2270–2305. [PubMed: 15026373]

Valdman A, Fang X, Pang ST, Ekman P, Egevad L. Prostate. 2004; 60:367–371. [PubMed: 15264249]

van Lohuizen M, Verbeek S, Krimpenfort P, Domen J, Saris C, Radaszkiewicz T, Berns A. Cell. 1989; 56:673–682. [PubMed: 2537153]

Vias M, Massie CE, East P, Scott H, Warren A, Zhou Z, Nikitin AY, Neal DE, Mills IG. BMC Med Genomics. 2008; 1:17. [PubMed: 18489756]

Wafa LA, Palmer J, Fazli L, Hurtado-Coll A, Bell RH, Nelson CC, Gleave ME, Cox ME, Rennie PS. Hum Pathol. 2007; 38:161–170. [PubMed: 16997353]

Wang Z, Bhattacharya N, Mixter PF, Wei W, Sedivy J, Magnuson NS. Biochim Biophys Acta. 2002; 1593:45–55. [PubMed: 12431783]

Xin L, Ide H, Kim Y, Dubey P, Witte ON. Proc Natl Acad Sci U S A. 2003; 100(Suppl 1):11896–11903. [PubMed: 12909713]

Yeh E, Cunningham M, Arnold H, Chasse D, Monteith T, Ivaldi G, Hahn WC, Stukenberg PT, Shenolikar S, Uchida T, Counter CM, Nevins JR, Means AR, Sears R. Nat Cell Biol. 2004; 6:308–318. [PubMed: 15048125]

Yuan TC, Veeramani S, Lin MF. Endocr Relat Cancer. 2007; 14:531–547. [PubMed: 17914087]

Zhang XQ, Kondrikov D, Yuan TC, Lin FF, Hansen J, Lin MF. Oncogene. 2003; 22:6704–6716. [PubMed: 14555984]

Zhang Y, Wang Z, Li X, Magnuson NS. Oncogene. 2008; 27:4809–4819. [PubMed: 18438430]

Zhou Z, Flesken-Nikitin A, Corney DC, Wang W, Goodrich DW, Roy-Burman P, Nikitin AY. Cancer Res. 2006; 66:7889–7898. [PubMed: 16912162]

Zippo A, De Robertis A, Serafini R, Oliviero S. Nat Cell Biol. 2007; 9:932–944. [PubMed: 17643117]

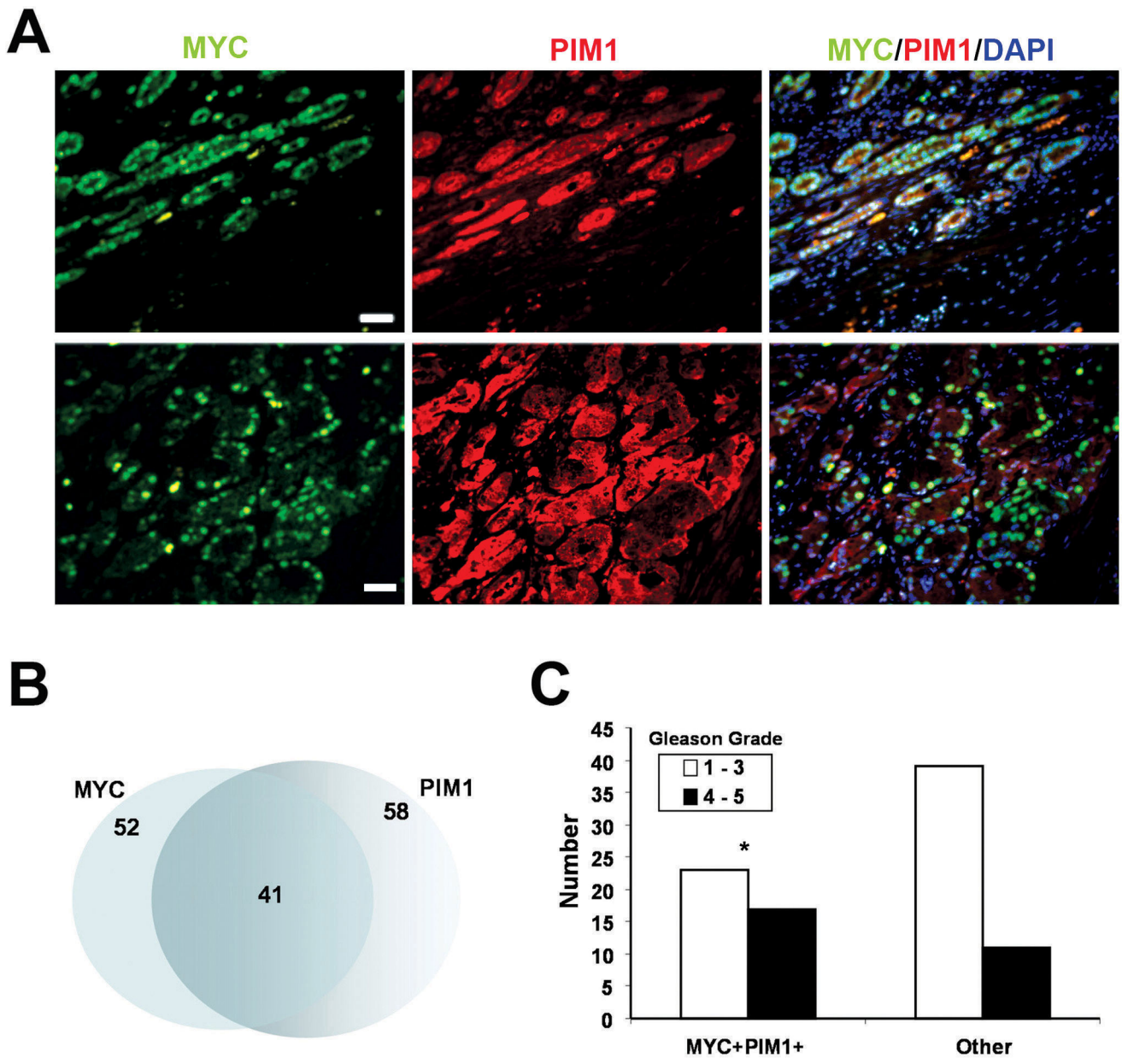

Figure 1.

Coexpression of c-MYC and PIM1 in human prostate tumors. ***A***, Representative micrographs of human prostate tumor samples showing co-expression of c-MYC (green) and PIM1 (red) by double immunofluorescence staining. DAPI was used as a nuclear counter stain. ***B***, Venn diagram showing overlap between samples positive for c-MYC and PIM1 overexpression. ***C***, Gleason grade distribution of samples coexpressing MYC and PIM1 (MYC+PIM1+) compared to samples without coexpression of MYC and PIM1 (other). MYC+PIM1+ samples are associated with higher Gleason grades. *P < 0.05.

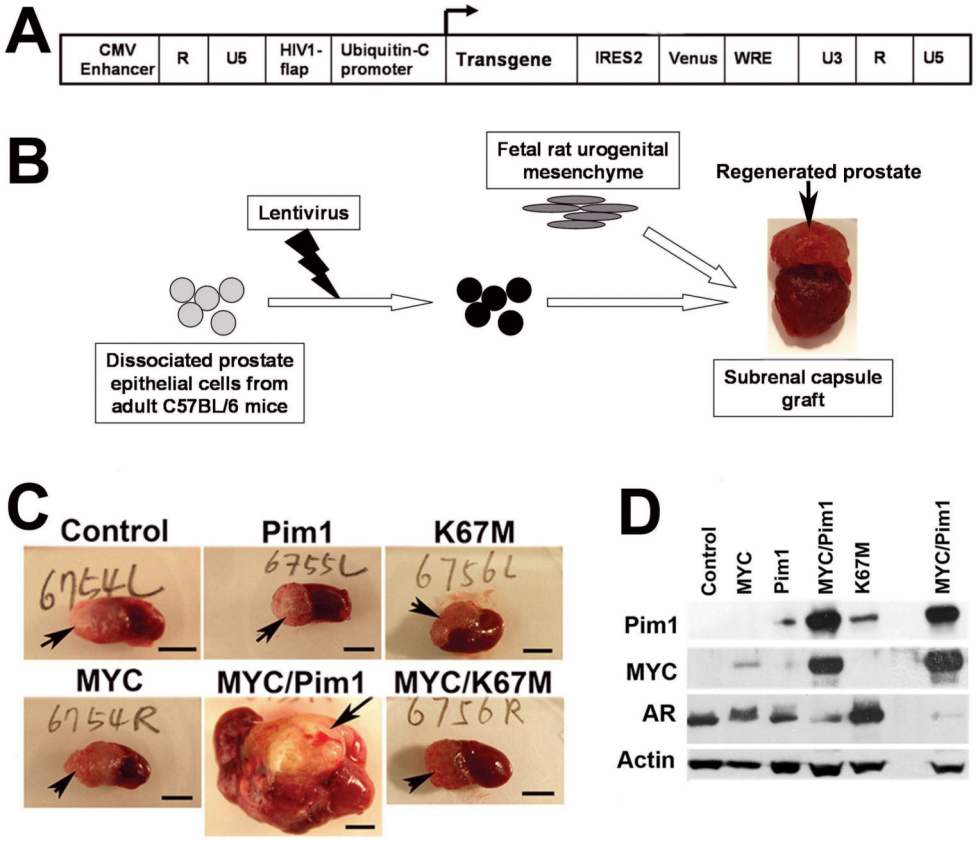

Figure 2.

Tissue recombination coupled with lentiviral-mediated gene transfer for expression of MYC and Pim1 in regenerated mouse prostate. ***A***, Schematic of the bicistronic lentiviral vector FM-1 used to target transgene expression together with YFP/Venus. ***B***, Scheme used for prostate recombination. Primary mouse prostate epithelial cells were infected with the indicated lentiviruses and recombined with fetal rat urogenital mesenchyme to regenerate prostates. ***C***, Representative images of sub-renal capsule grafts (arrows) after 6 weeks. Scale bar, 5mm. ***D***, Western blot analyses from 6-week graft tissue lysates with the indicated antibodies.

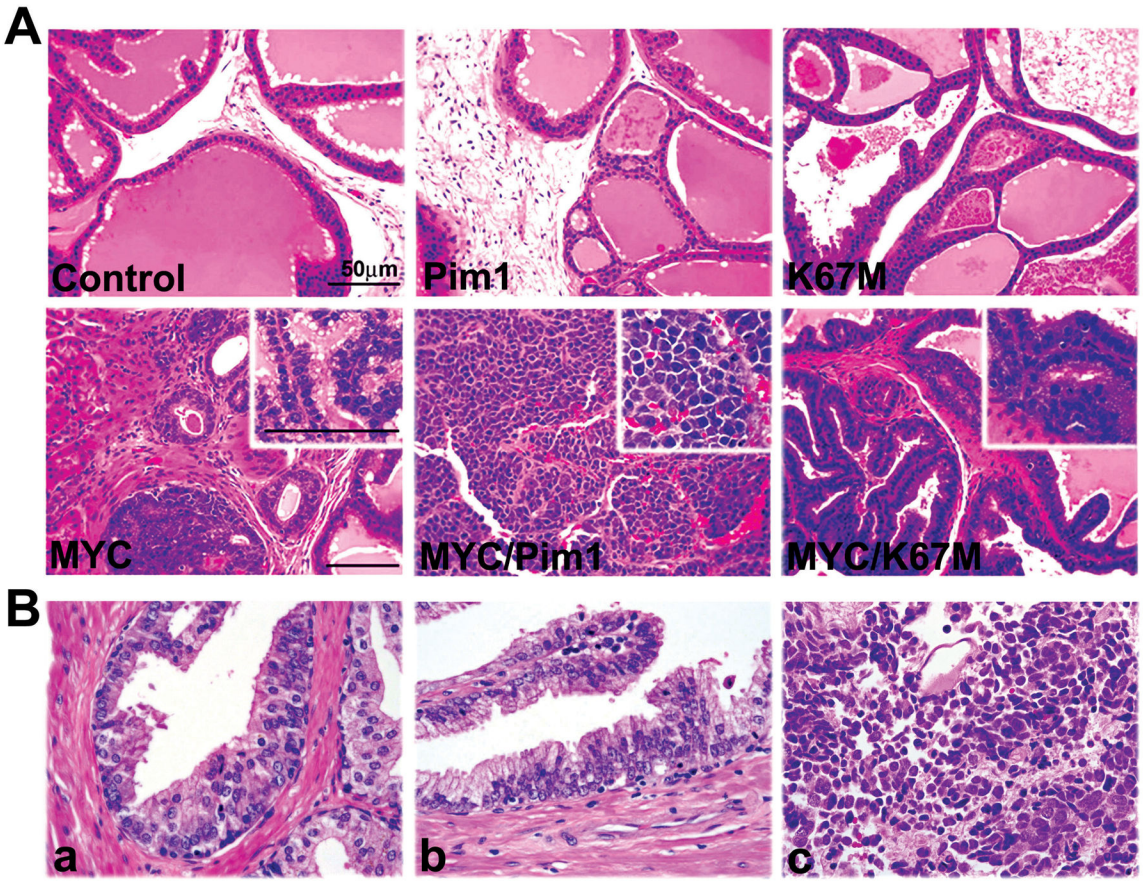

Figure 3.

MYC/Pim1 coexpression leads to high-grade prostate cancer within 6 weeks. ***A***, H&E stained sections of 6-week grafts show normal-looking prostatic glands in control, Pim1 and K67M grafts. MYC and MYC/K67M samples show HGPIN lesions and hypercellular stroma. The MYC/Pim1 samples show high-grade tumor consistent with neuroendocrine carcinoma. Scale bar, 50 μm. Insets: Higher-magnification images. ***B***, Human prostate samples showing LGPIN (a), HGPIN (b) and neuroendocrine (small cell) carcinoma (c) are shown for comaparison. The small cell carcinoma shows classic features of this tumor type with nuclear molding, focal “salt and pepper” nuclei, and abundant nuclear debris and apoptosis. (Original magnifications for a and b 600×; c, 400×).

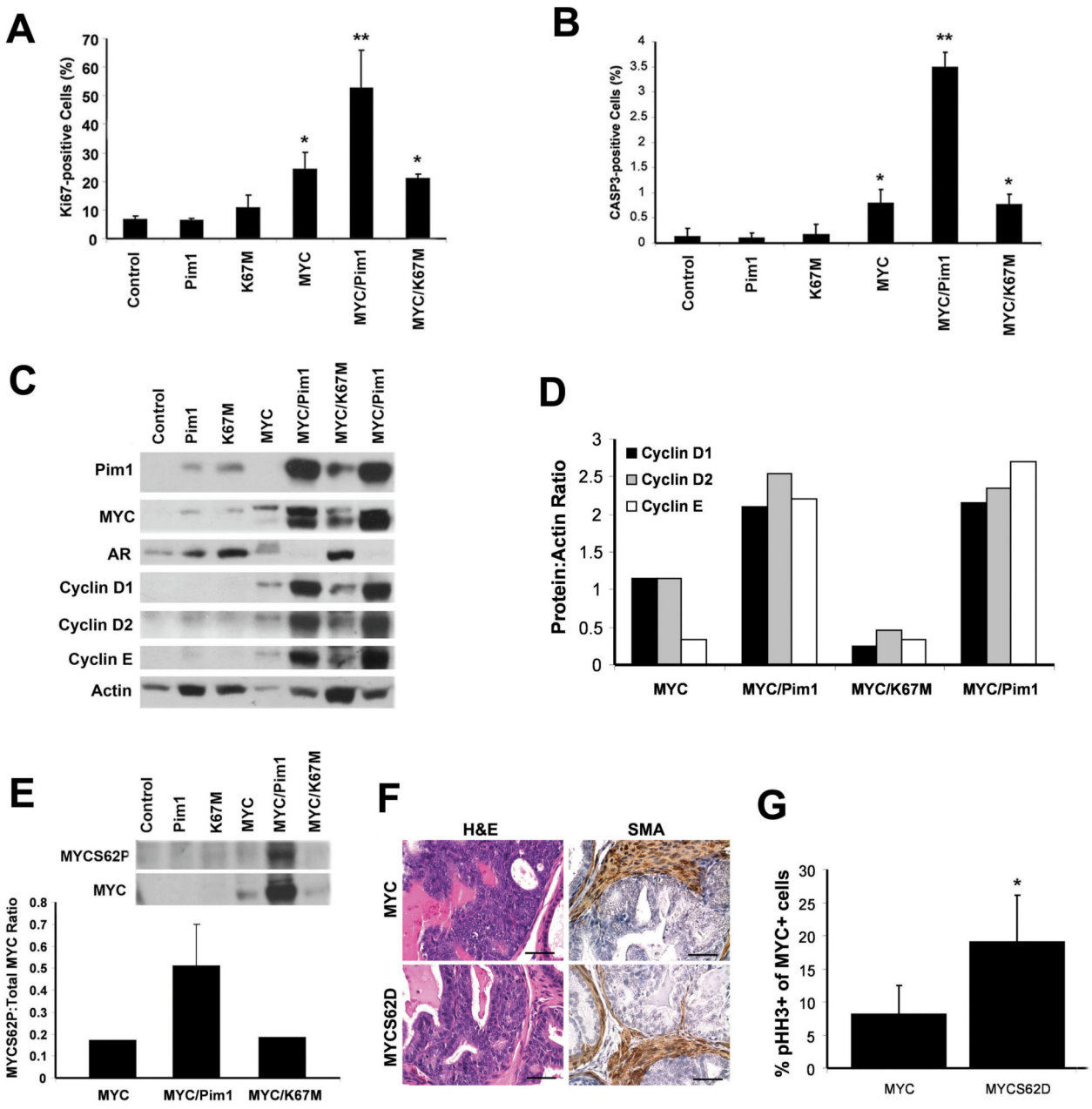

Figure 4.

Increased cellular proliferation and MYC activity in MYC/Pim1 tumors. ***A***, Ki67 proliferative index in graft tissues. ***B***, Apoptotic index in graft tissues determined by staining for activated caspase 3. Data shown as mean ± SD, N=3. *, $P < 0.05$ relative to control. **, $P < 0.05$ relative to all samples. ***C***, Western blot for the indicated proteins in graft tissue lysates. ***D***, Quantitation of Cyclins D1, D2 and E levels from "C" normalized to actin. ***E,*** Upper panel: Western blot for serine-62 phosphorylated MYC (MYCS62P) and total MYC. Lower panel: Quantitation of western blot data. ***F,*** Six-week grafts expressing the MYCS62D phosphomimetic mutant are similar by H&E and SMA staining to wild type MYC grafts. Scale bars, 50 μm. ***G***, Higher mitotic index (% phospho-histone H3 positive

MYC-expressing cells) in grafts expressing the MYCS62D mutant (n=4) compared to those expressing wild type MYC (n=5). *, $P < 0.05$.

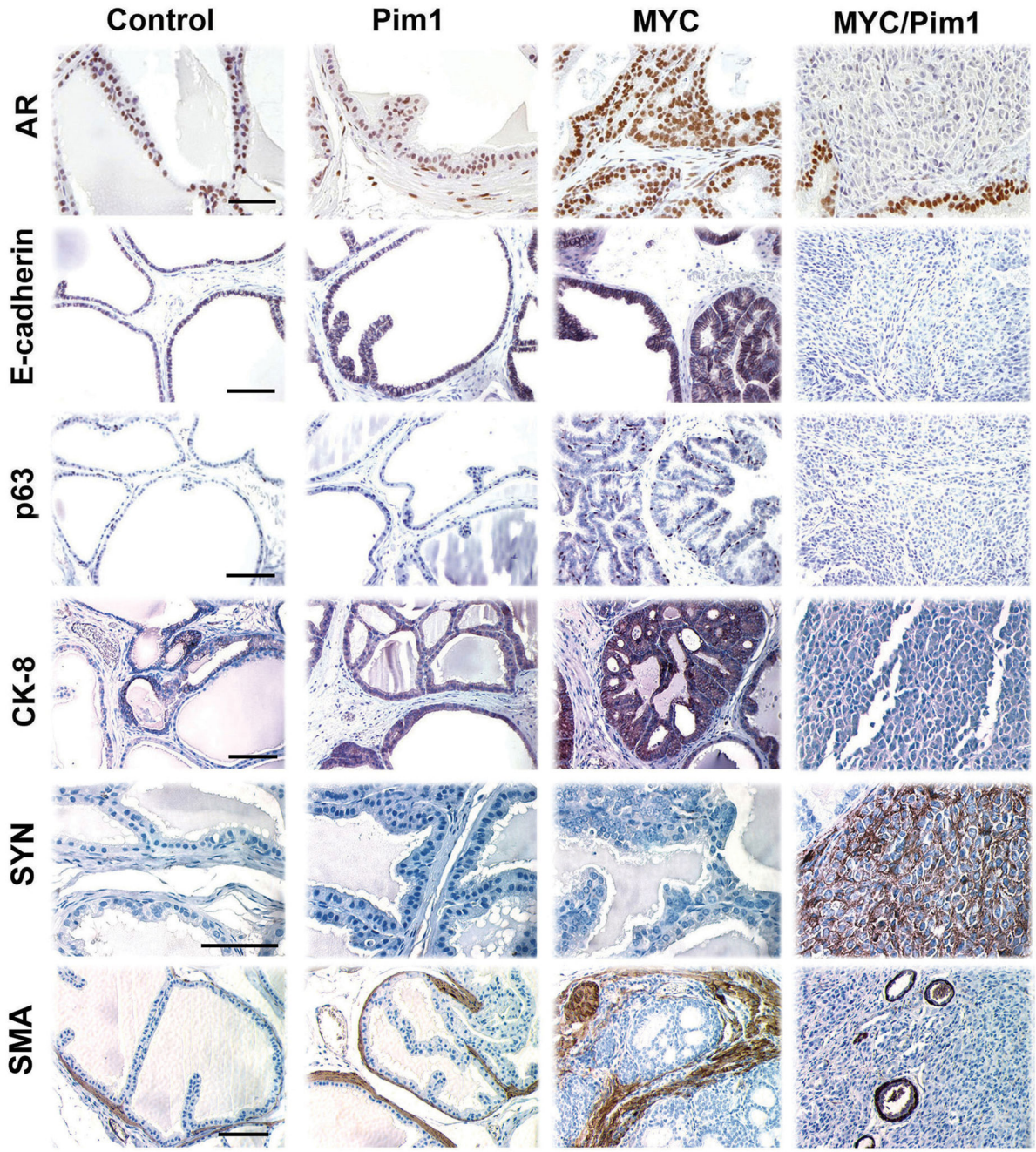

Figure 5.

MYC/Pim1 coexpression shows evidence of neuroendocrine (NE) differentiation. Immunohistochemical analysis of 6-week tissue recombinants for expression of androgen receptor (AR), E-cadherin, p63, cytokeratin 8 (CK8), synaptophysin (SYN) and smooth muscle actin (SMA). MYC/Pim1 tumors showed reduced expression of AR, E-cadherin, p63 and CK8 expression and strong expression of synaptophysin. HGPIN lesions in MYC group strongly express SMA in the hypercellular stroma. Note loss of SMA staining in the MYC/

Pim1 tumors, consistent with their invasive nature. SMA positive cells surrounding blood vessels in MYC/Pim1 tumor served as internal positive controls. Scale bars, 50 μm.

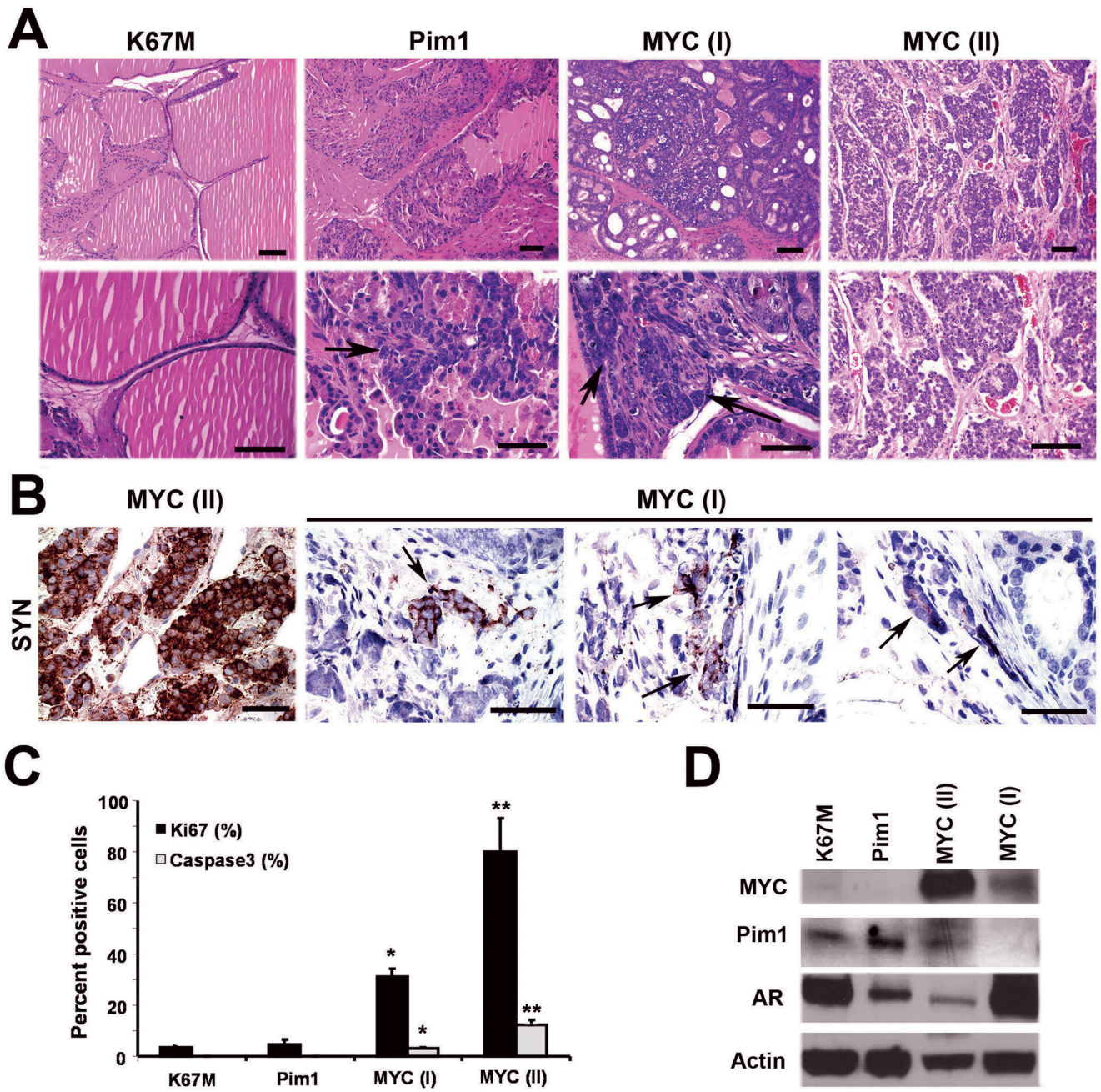

Figure 6.

Chronic (12-week) overexpression of Pim1 results in LGPIN while MYC expression leads to a combination of adenocarcinoma and carcinoma with neuroendocrine differentiation. ***A***, H&E sections show normal-looking prostate glands in K67M grafts and epithelial hyperplasia and LGPIN (arrow) in Pim1 grafts. Twelve-week MYC grafts resulted in two types of lesions: MYC (I) showed HGPIN with invasive adenocarcinoma (arrows), while MYC (II) had high-grade tumor consistent with neuroendocrine carcinoma. N=3 each. Scale bars, 50 μm. ***B***, Immunohistochemistry for synaptophysin (SYN) shows strong expression in MYC (II) neuroendocrine tumor and isolated focal expression (arrows) in MYC (I)

adenocarcinoma. Scale bars, 50 μm. ***C***, Proliferative (Ki67) and apoptotic (activated caspase 3) indices in 12-week graft tissues. *, P <0.05 relative to K67M or Pim1. **, P < 0.05 relative to all other groups. N=3. ***D***, Western blot analyses for the indicated proteins in 12-week graft tissues. Note increased Pim1 and reduced AR expression in MYC (II) sample.

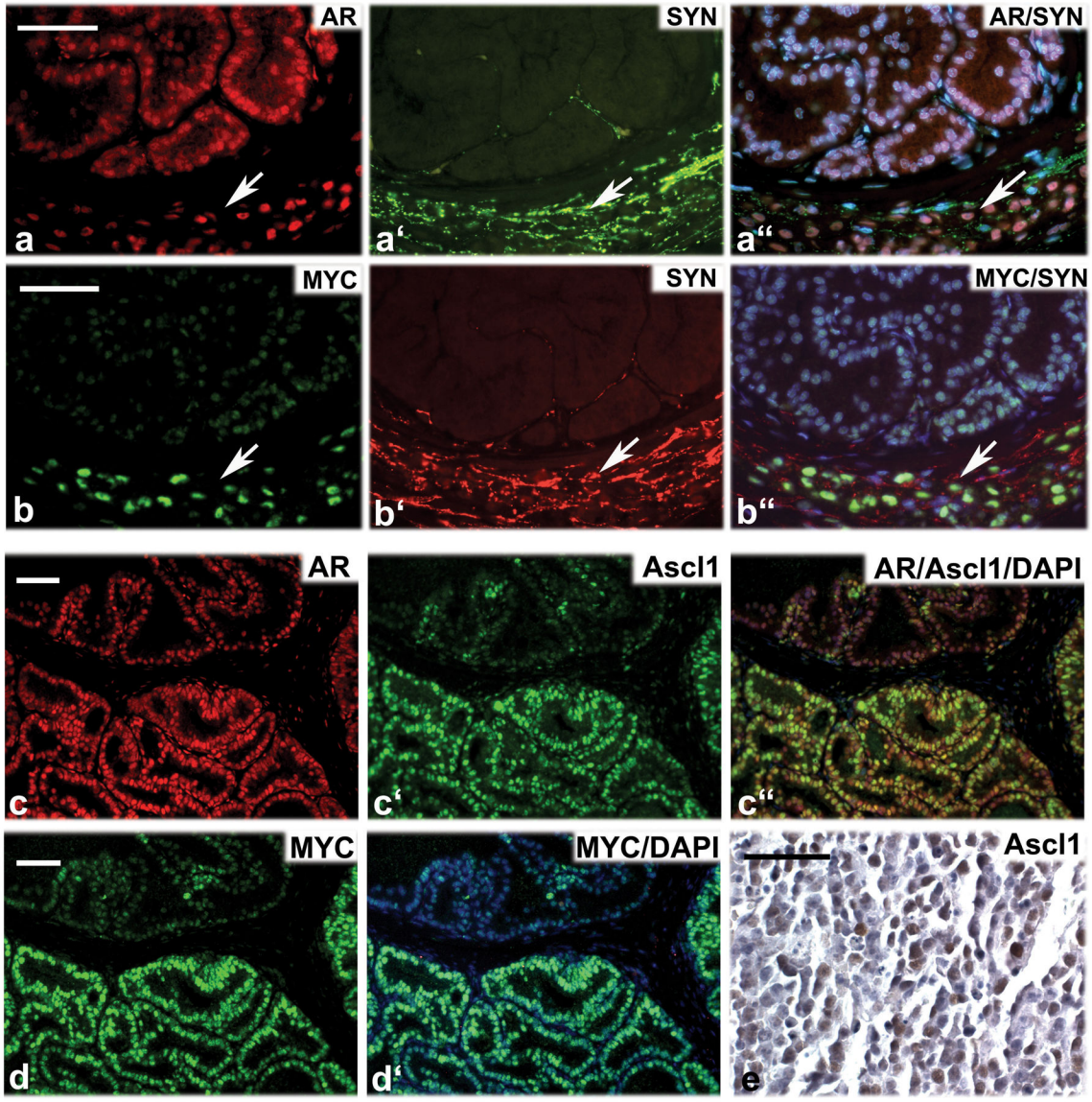

Figure 7.

Evidence that c-MYC/Pim1-induced neuroendocrine tumors arise by transdifferentiation. ***a-a"***, MYC/Pim1 graft costained for androgen receptor (AR, red), synaptophysin (SYN, green) and DNA (DAPI, blue). ***b-b"***, An adjacent section to that in '***a***' stained for MYC (green), synaptophysin (SYN, red) and DNA (DAPI, blue). Arrows point to nest of tumor cells coexpressing AR, SYN and MYC. ***c-c"***, MYC/Pim1 graft costained for androgen receptor (AR, red), synaptophysin (Ascl1, green) and DNA (DAPI, blue). ***d*** and ***d',*** An adjacent section to that in '***c'*** stained for MYC (green), and DNA (DAPI, blue). Note coexpression of AR, Ascl1 and MYC. ***d"***, Ascl1 expression (brown) in a MYC/Pim1 neuroendocrine tumor. Scale bars, 50 μm.